DOI 10.1515/hsz-2012-0202 — Biol. Chem. 2012; 394(1): 113–123

Radoslaw Szmyd[a], Anna Grazyna Goralczyk[a], Lukasz Skalniak, Agnieszka Cierniak, Barbara Lipert, Francesca Larese Filon, Matteo Crosera, Julia Borowczyk, Eliza Laczna, Justyna Drukala, Andrzej Klein and Jolanta Jura*

Effect of silver nanoparticles on human primary keratinocytes

Abstract: Silver nanoparticles (AgNPs) have many biological applications in biomedicine, biotechnology and other life sciences. Depending on the size, shape and the type of carrier, AgNPs demonstrate different physical and chemical properties. AgNPs have strong antimicrobial, antiviral and antifungal activity, thus they are used extensively in a range of medical settings, particularly in wound dressings but also in cosmetics. This study was undertaken to examine the potential toxic effects of 15 nm polyvinylpyrrolidone-coated AgNPs on primary normal human epidermal keratinocytes (NHEK). Cells were treated with different concentrations of AgNPs and then cell viability, metabolic activity and other biological and biochemical aspects of keratinocytes functioning were studied. We observed that AgNPs decrease keratinocyte viability, metabolism and also proliferatory and migratory potential of these cells. Moreover, longer exposure resulted in activation of caspase 3/7 and DNA damage. Our studies show for the first time, that AgNPs may present possible danger for primary keratinocytes, concerning activation of genotoxic and cytotoxic processes depending on the concentration.

Keywords: caspase activation; cell viability; MAP kinase activation; migration; primary keratinocytes; silver nanoparticles.

[a] These authors contributed equally to this work.
***Corresponding author: Jolanta Jura,** Department of General Biochemistry, Faculty of Biochemistry, Biophysics and Biotechnology, Jagiellonian University, 30-387 Krakow, Poland, e-mail: jolanta.jura@uj.edu.pl
Radoslaw Szmyd: Department of General Biochemistry, Faculty of Biochemistry, Biophysics and Biotechnology, Jagiellonian University, 30-387 Krakow, Poland
Anna Grazyna Goralczyk: Department of General Biochemistry, Faculty of Biochemistry, Biophysics and Biotechnology, Jagiellonian University, 30-387 Krakow, Poland
Lukasz Skalniak: Department of General Biochemistry, Faculty of Biochemistry, Biophysics and Biotechnology, Jagiellonian University, 30-387 Krakow, Poland
Agnieszka Cierniak: Department of General Biochemistry, Faculty of Biochemistry, Biophysics and Biotechnology, Jagiellonian University, 30-387 Krakow, Poland
Barbara Lipert: Department of General Biochemistry, Faculty of Biochemistry, Biophysics and Biotechnology, Jagiellonian University, 30-387 Krakow, Poland
Francesca Larese Filon: Unit of Occupational Medicine, University of Trieste, 34129 Trieste, Italy
Matteo Crosera: Department of Chemical and Pharmaceutical Sciences, University of Trieste, 34127 Trieste, Italy
Julia Borowczyk: Department of General Biochemistry, Faculty of Biochemistry, Biophysics and Biotechnology, Jagiellonian University, 30-387 Krakow, Poland
Eliza Laczna: Department of General Biochemistry, Faculty of Biochemistry, Biophysics and Biotechnology, Jagiellonian University, 30-387 Krakow, Poland
Justyna Drukala: Department of General Biochemistry, Faculty of Biochemistry, Biophysics and Biotechnology, Jagiellonian University, 30-387 Krakow, Poland
Andrzej Klein: Department of General Biochemistry, Faculty of Biochemistry, Biophysics and Biotechnology, Jagiellonian University, 30-387 Krakow, Poland

Introduction

Nanoparticles are of great scientific interest because of the wide variety of potential applications. There is a growing list of reports concerning applications of nanoparticles in biomedicine, biotechnology and cosmetology. Because of strong antimicrobial, antiviral and antifungal activity (Edwards-Jones, 2009), silver nanoparticles (AgNPs) have been used extensively in medical and healthcare sectors (Benn and Westerhoff, 2008; Li et al., 2011; Teow et al., 2011). They are used as anti-pathogenic additives in products such as wound dressings, surgical instruments, cleaning products, cosmetics and cloths. Nanoparticles incorporated to these products come in a direct contact with skin and may affect the biology of epidermal cells (Chen and Schluesener, 2008; Ahamed et al., 2010; Teow et al., 2011).

Although the data on the effect of AgNPs on various cell types are often not consistent, it is now clear that different surface chemistry and size of nanoparticles are some of the most important parameters, which must be included when considering their unique properties. For example, Liu and co-workers (2010) tested the impact of 5, 20 and 50 nm AgNPs on cell lines derived from different human organs

(lung adenocarcinoma epithelial cells, stomach cancer cells, hepatocellular carcinoma cells, and breast adenocarcinoma cells). They observed that smaller nanoparticles enter the cells more easily than the larger ones and have a more significant effect on membrane integrity, the level of reactive oxygen species (ROS) and induction of apoptosis and cell cycle arrest. Generally, it seems that silver nanoparticles of <50 nm diameter are more deleterious for cells, decreasing cell metabolism and inducing cytotoxic and genotoxic effects (Liu et al., 2010; Park et al., 2011; Kim et al., 2012).

Differences in the level of toxicity of AgNPs also depend on the type of polymer surfactants, which are used to stabilize nanoparticles. In the work of Lin et al. (2012), three types of polymer stabilizers were tested: poly(oxyethylene)-segmented imide (POEM); poly(styrene-co-maleic anhydride)-grafting poly(oxyalkylene) (SMA); and poly(vinyl alcohol) (PVA). Each of them displayed a different level of toxicity. Another protective agent frequently used in medicine is polyvinylpyrrolidone (PVP). It would appear not to be toxic and does not irritate or induce sensitization when applied to the skin (Das et al., 2008). Despite that, it is obvious now that more detailed studies are necessary to determine all potential side-effects of AgNPs.

This study was undertaken to examine the potential toxic effects of 15 nm polyvinylpyrrolidone-coated (PVP) silver nanoparticles on human primary keratinocytes. We decided to use 15 nm AgNPs, because it is one of the smallest sizes on the market and is commonly used in typical dressings prepared by various companies (Chaloupka et al., 2010). The data on the impact of silver nanoparticles on primary keratinocytes is limited in the literature, although these cells should be tested more carefully and intensively. This is because wound dressings, clothes, disinfecting sprays and creams containing AgNPs are now commonly used in skin care. As keratinocytes constitute 90% of the epidermis, they are probably the most frequently exposed to the mentioned forms of commercially available AgNPs.

In our study, cells were treated with different concentrations of 15 nm PVP-coated AgNPs and then cell morphology, viability and metabolic activity were studied. Furthermore we analysed the effect of AgNPs on integrity of keratinocytes genome, cellular stress as well as activation of apoptotic processes.

Results

Effect of AgNPs on cell viability

The cytotoxic effects of AgNPs were examined by a combination of two assays – ATP content assay and MTT assay. This allowed us to monitor cell metabolic activity and growth effects. Experiments were carried out using four concentrations of AgNPs: 6.25, 12.5, 25 and 50 μg/ml. Untreated cells served as a control. As shown in Figure 1A in the ATP content assay we observed a dose- and time-dependent decrease in luminescence intensity in NHEKs. Around a 40% decrease in ATP content was observed for cells exposed to a 6.25 μg/ml concentration of AgNPs, but in the case of 50 μg/ml concentration the content of ATP decreased by almost 80%. The changes were even more pronounced after 48 h of AgNPs treatment (Figure 1A).

The MTT assay showed a concentration-dependent decrease in cell viability only after 24 h of exposure to AgNPs. We did not observe significant changes in cell viability for the lowest concentration (6.25 μg/ml), whereas cell viability decreased by more than 30% in case of cells treated with the highest concentration (50 μg/ml; Figure. 1B). No concentration-dependent changes in cell viability were observed after 48 h of exposure, however all AgNP concentrations caused around a 50% decrease in cell viability in comparison to the control (Figure 1B).

In order to further analyse the influence of AgNPs on NHEKs, a BrdU incorporation assay was performed to investigate the rate of cell proliferation. Cells treated with AgNPs showed a concentration-dependent decrease in the proliferation rate after 24 h of exposure (Figure 1C). The proliferation rate decreased to almost 50% in cells treated with the 50 μg/ml concentration of nanoparticles. After 48 h we observed a further decrease in proliferation rate (by up to 70%) but reaching the same level for all used concentrations of AgPNs, similarly to the MTT assay (Figure 1A). Performing these tests we noticed that the use of the 50 μg/ml concentration causes aggregation of nanoparticles thus, we did not use it in further experiments.

Activation of apoptosis by AgNPs

The effect of AgNPs on activation of apoptosis in keratinocytes was verified by the determination of caspases 3 and 7 activity. No changes were observed after 24 h exposure (data not presented). However, concentration-dependent increase in caspases 3 and 7 activity was observed after 48 h. In comparison to the control sample, we observed a 1.7-fold increase for the 12.5 μg/ml concentration of AgNPs and a 2.5-fold increase for the 25 μg/ml concentration (Figure 1D). We did not observe significant changes in caspase 3/7 activity when the lowest concentration (6.25 μg/ml) was used (data not shown).

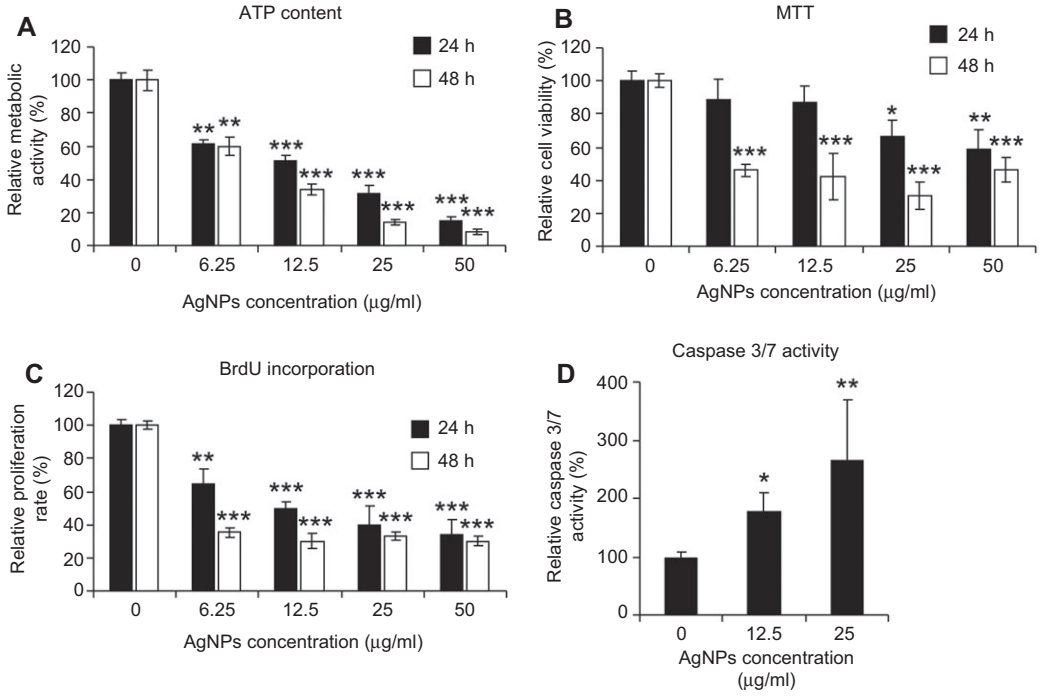

Figure 1 Effects of AgNPs on the biology of primary keratinocytes.
(A) Metabolic activity of NHEKs exposed to AgNPs. Intracellular ATP content was measured to determine metabolic cell condition. NHEKs (plated at the density of 4×10^3 per well of 96-well plates) were treated with different concentrations of AgNPs for 24 h and 48 h. Untreated cells served as a control. For statistics, a Student's *t*-test was performed (*$p<0.05$; **$p<0.01$; ***$p<0.001$). This graph represents the mean±SD of three independent experiments, each performed in triplicate (number of wells=9). (B) Viability of NHEKs exposed to AgNPs. Cell viability was analysed using MTT assay. NHEKs (plated at the density of 4×10^3 per well of 96-well plates) were treated with different concentrations of AgNPs for 24 h and 48 h. Untreated cells served as a control. For statistics, a Student's *t*-test was performed (*$p<0.05$; **$p<0.01$; ***$p<0.001$). This graph represents the mean±SD of four independent experiments, each performed in quintuplicate (number of wells=20). (C) Proliferation rate (BrdU assay) of NHEKs exposed to AgNPs. NHEKs (plated at the density of 3×10^3 per well of 96-well plates) were treated with indicated concentrations of AgNPs for 24 h and 48 h. Cells were incubated with BrdU labeling solution for 12 h. Untreated cells served as a control. For statistics, a Student's *t*-test was performed (*$p<0.05$; **$p<0.01$; ***$p<0.001$). This graph represents the mean±SD of three independent experiments, each performed in triplicate (number of wells=9). (D) Apoptotic cell death measured by the determination of caspase 3/7 activity. The luminescent assay for caspase 3/7 activity was performed using 3 μg of total protein isolated from NHEKs after incubation with 12.5 and 25 μg/ml AgNPs for 48 h. For statistics, a Student's *t*-test was performed (*$p<0.05$; **$p<0.01$; ***$p<0.001$). This graph represents the mean±SD from three independent experiments, each performed in duplicate (number of wells=6).

Cell migration

The analysis of AgNPs influence on two-dimensional keratinocytes migration was performed by the time-lapse monitoring of cell movement. We observed significant inhibition of cell migration only in the samples treated for 24 h with 25 μg/ml concentration of AgNPs. The value of velocity of cell movement decreased about 30% compared to the control conditions. Lower concentration of nanoparticles (12.5 μg/ml) used in the experiment for the same time did not significantly affect cell movement (2.4 vs. 2.2 μm/min). However, more significant changes were observed for both concentrations when samples were incubated with AgNPs for 48 h. The lower concentration (12.5 ug/ml) resulted in around 40% cell motility inhibition and a higher concentration further decreased cell movement by up to 60% in comparison to the control (Figure 2). Similarly as per the caspase 3/7 activity assay, we did not observe significant changes in cell migration when the lowest concentration (6.25 μg/ml) was used (data not shown).

Genomic instability

Quantitation of DNA strand breaks was performed using single cell gel electrophoresis (comet assay) and the breaks presence was assessed by the evaluation of DNA in a tail of a comet. As we did not see the effect of the lowest concentration of AgNPs (6.25 μg/ml) on cells in this experiment, NHEKs were exposed only to a concentration of AgNPs at 12.5 and 25 μg/ml for 24 h and 48 h. Untreated

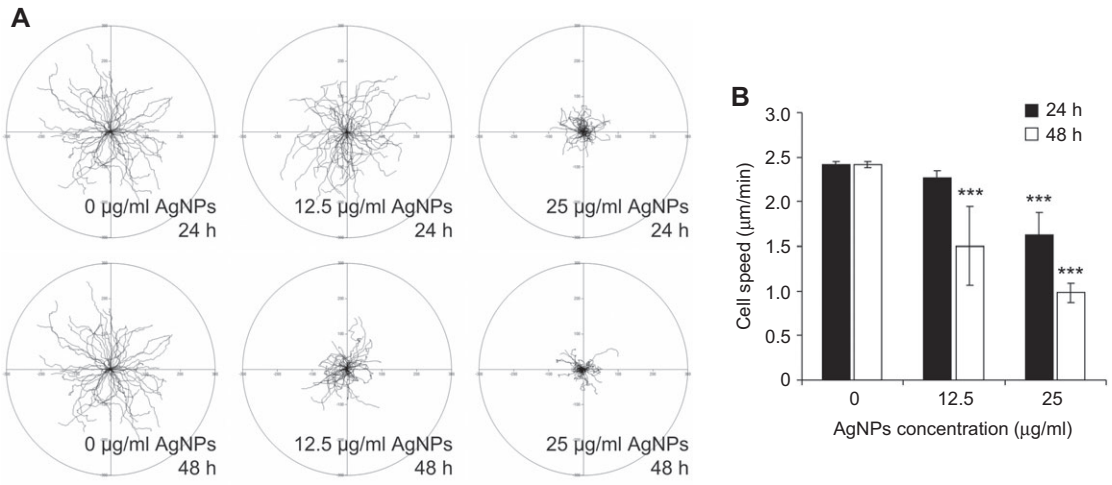

Figure 2 Effect of AgPNs on cell migration.
Cell migration was examined with a Leica DMI6000B microscope equipped with LAS AF software. NHEKs were plated in 6-well culture plates at the density of 4×10^4 per well and treated with 12.5 and 25 µg/ml AgNPs. Cell movements were recorded 24 h and 48 h after AgNPs addition for 90 min with a time-lapse of 1.5 min. (A) The tracks of individual cells were determined from the series of changes in the cell central positions, pooled and analysed to determinate the total length of the cell trajectory (TLCT). (B) All analyses were performed using Hiro software v.1.0.0.4. Presented data are mean±SD from cell speed values for 150 cells, measured in three independent experiments. A Student's *t*-test was carried out for statistics (*$p<0.05$; **$p<0.01$; ***$p<0.001$).

cells served as a control. As shown in Figure 3 the use of 25 µg/ml of AgNPs resulted in a significant increase in DNA damage both at 24 and 48 h of treatment. After 24 h, 25% of DNA was present in the comet tail, while 48-h incubation resulted in the augmentation of the DNA comet formation reaching a level of 33%.

Signaling pathways

The influence of AgNPs on signal-transduction pathways was investigated by determining the phosphorylation of p38, ERK and JNK MAP kinases, as well as AKT kinase and p53 protein. Our results demonstrated that p38, ERK1/2 and p53 phosphorylation level was increased. Up-regulation of p38 was observed for both concentrations (12.5 µg/ml and 25 µg/ml) but was significantly stronger for higher concentrations. The activation was visible after 30 min of AgNPs treatment and subsequently reduced to the basal level after 4 h regardless of the AgNPs concentration (Figure 4). Considerably weaker was phosporylation of ERK1/2 and p53. Moreover, we did not see any differences in the case of JNK and AKT phosphorylation level.

Gene expression analysis

To explore possible molecular mechanisms of AgNPs-mediated cell death, we measured changes in the level of transcripts encoding selected proteins involved in the apoptosis pathway. From activators of apoptosis we analysed Bak1, Bax, Bbc (PUMA), and p53. We decided also to measure the mRNA level of the Bcl-2 protein, as it is a key inhibitor of apoptosis. We assessed mRNA isolated from NHEKs stimulated with AgNPs in concentrations of 12.5 and 25 µg/ml. Expression of selected transcripts was measured at 4, 12, and 24 h after AgNPs addition.

Levels of transcripts coding for Bak1, p53 and Bcl-2 were not disturbed by AgNPs treatment at any time. In contrast, mRNAs coding for Bax and PUMA were up-regulated by AgNPs. In the case of Bax, up-regulation was observed only for the 25 µg/ml concentration of AgNPs and reached 1.5-fold increase compared to the control. The level of PUMA mRNA was also increased 1.5 fold and peaked at 12 h of stimulation with a lower concentration of AgNPs. However, stimulation with a higher concentration (25 µg/ml) resulted in almost the same up-regulation but after only 4 h of stimulation. Then, after longer stimulation the transcript level was decreased, subsequently to the level comparable with the control (Figure 5).

Discussion

Nanoparticles are defined as structures, that have at least one dimension in the 1–100 nm range. Their ultra-small size in comparison to enormous surface area makes

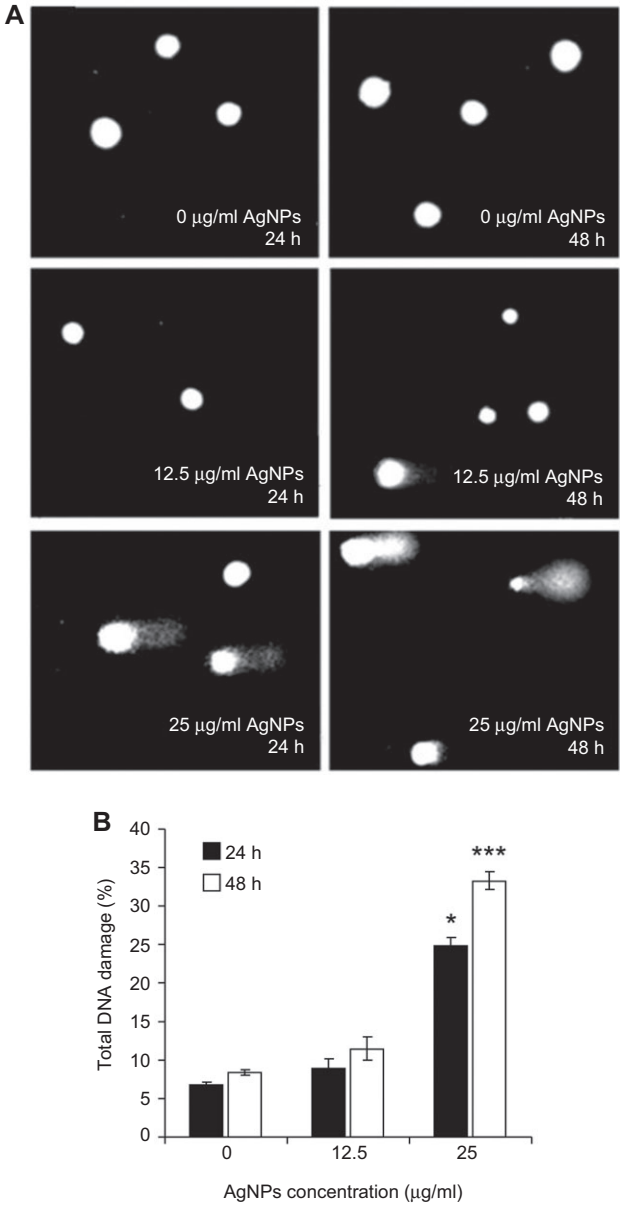

Figure 3 DNA damage in NHEKs verified by comet assay. NHEKs were plated at the density of 2.1×10^3 cells/cm^2. After 24 h, cells were treated with 12.5 and 25 μg/ml AgNPs for 24 h and 48 h. Untreated cells served as a control (A). DNA damage presented as the mean value of the percentage of DNA in the comet tail (%DNA). Images were made using the computer program Comet Plus (Theta System GmbH, Germany). (B). The graph represents the mean±SD of three independent experiments. In each experiment, total DNA damage was measured in 100 cells. Statistically significant differences were calculated using an RIR Tukey test (*$p<0.05$; ***$p<0.001$).

AgNPs very reactive forms. The small size also confers greater mobility of particles and has an impact on their cellular distribution. Depending on the size, shape and the type of a carrier, AgNPs demonstrate different physical and chemical properties. Despite the rapid development and common usage of AgNPs, relatively few researches have been executed to determine their biological impact on the cellular level.

In our study we decided to use PVP-coated AgPNs, as this type of polymer is generally considered to be safe and is increasingly widespread in medicine and foodstuffs. PVP is used as a binder in many pharmaceutical tablets. It is also used as a stabilizer in different foods (E1201) and in the wine industry as a fining agent for white wine. This chemical is approved for many uses (Inactive Ingredients in FDA Approved Drugs), thus we believe that when using PVP as a coating agent the observed toxic effects are limited to the toxicity of silver nonmaterial, not its envelope.

As AgNPs are present in many products used in skin care, keratinocytes are probably the cells most frequently exposed to these nanoparticles. AgNPs are incorporated not only in health care products, like cosmetics or textiles, but they also are commonly used in medical products, like wound dressings used in the treatment of wounds and burns (Chen and Schluesener, 2008). One of the important phases of wound healing is re-epithelialization. This phase involves multiple processes, one of which is the migration of epidermal keratinocytes from around the wound. Depending on the depth of the wound, the process starts within a few hours to 2 days after wounding (Hackam and Ford, 2002; Bartkova et al., 2003; Henry et al., 2003). Besides migration, the proliferation phase starting soon after wounding, is also important in the efficient restoration of skin integrity.

As we have shown in our *in vitro* study, both processes essential for proper functioning of epidermal cells – migration and proliferation – are impaired following the exposure of human primary keratinocytes to 15 nm PVP-coated AgNPs. We observed that, depending on their concentration, AgNPs significantly decreased keratinocytes viability. Importantly, impaired condition resulted in the decrease of both migratory and proliferative properties of these cells. Loss of these properties was dose-dependent after 24 h incubation. Prolonged incubation with AgNPs gave a very significant decrease of cell survival but at the same level for all concentrations used in the experiment.

Moreover, we found that AgNPs toxicity was accompanied by the increase in caspase 3/7 activity. It was not visible after 24 h but we observed significant and dose-dependent up-regulation after 48 h of the experiment. Several reports show that AgNPs trigger dose-dependent cytotoxicity of other type of cells through activation of the caspase 3 enzyme, leading to induction of apoptosis (Arora et al., 2009; Kalishwaralal et al., 2009; Sriram et al., 2010). One of the effects of activation of apoptosis,

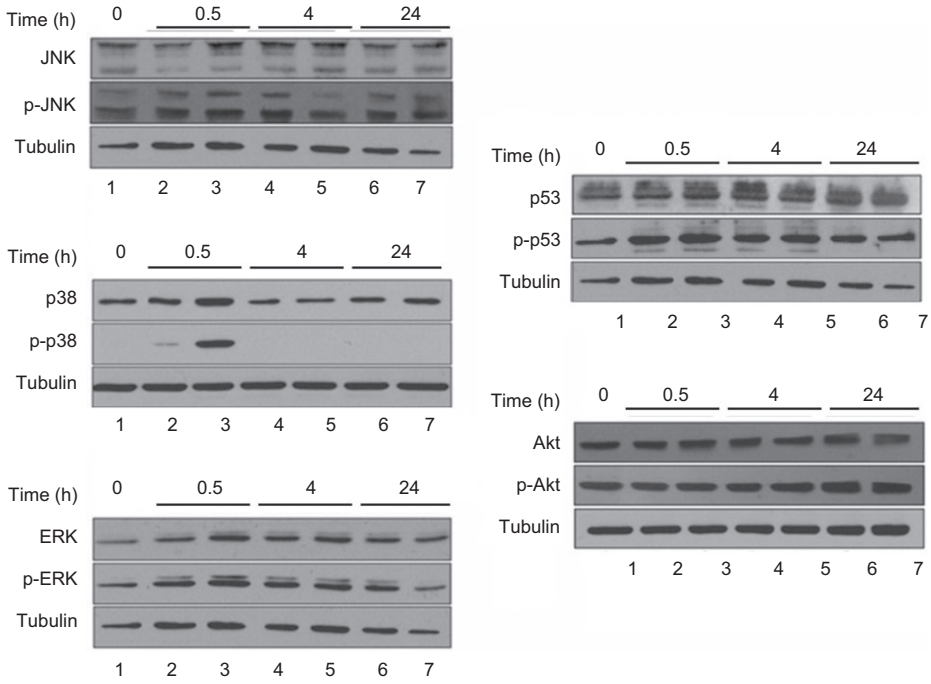

Figure 4 The activation of ERK, p38, JNK, AKT and p53 verified by Western blot analysis.
NHEKs were cultured in 60-mm tissue culture dishes at density of 9.5×10^3 cells/cm^2. The cells were exposed to 12.5 μg/ml (lines 2, 4 and 6) or 25 μg/ml (lines 3, 5 and 7) AgNPs for the indicated periods of time. Untreated cells were used as a control (line 1). Tubulin was used as an internal control to monitor for equal loading. These blots are representative of three independent experiments.

but also the marker of this process, is DNA fragmentation. We showed dose-dependent increase in the rate of DNA breaks. There are reports that AgNPs activate ROS production, which results in the initiation of DNA breaks but also in the damage of other cellular organelles and components (Piao et al., 2010; Asare et al., 2011; Ma et al., 2011).

One of the signals of cellular response to toxins or physical stresses is activation of selected protein kinases, essential in signal transduction towards appropriate transcription factors. We analysed the activity of p38, ERK, JNK and AKT kinases, as well as the activity of p53, a protein directly engaged in the regulation of DNA repair processes/

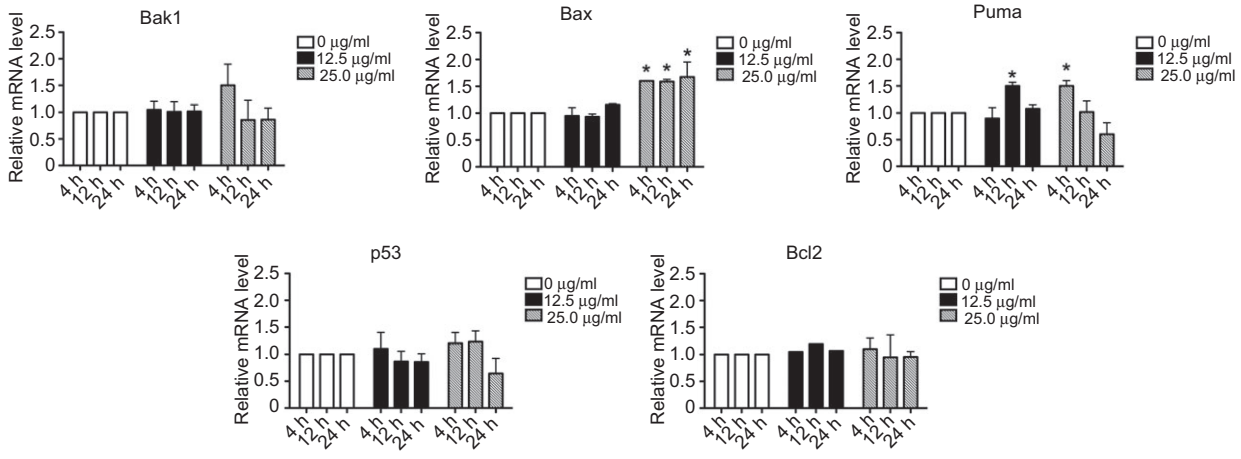

Figure 5 Expression of selected pro-apoptotic and anti-apoptotic genes in NHEKs.
Graphs show expression of Bak1, Bax, Bbc (PUMA), p53 and Bcl2 mRNAs in NHEKs treated with various concentrations of AgNPs (0, 12.5 and 25 μg/ml) for different times (4, 12 and 24 h). Specific mRNAs were normalized to B2M level and presented as relative units compared to the control. Data represent mean±SEM (n=3). The asterisk indicates significant difference between the treated sample and untreated control ($p<0.05$).

apoptosis. We observed only a temporary activation of p38 MAPK, weak activation of ERK1/2 and p53. Activation of p38 MAPK was also observed in a previous study (Eom and Choi, 2010), where the authors reported that AgNPs may induce toxic effects via Nrf-2 and NF-κB pathways. Besides, Lim and co-workers suggested that oxidative stress is an important mechanism in AgNPs-induced toxicity in *Caenorhabditis elegans* and PMK-1 p38 MAPK is involved in this phenomenon (Lim et al., 2012). There are also other reports that AKT (Kang et al., 2011) and JNK (Piao et al., 2010) kinases are activated by AgPNs. We did not see up-regulation of these kinases. It is possible that the level of stress triggered by nanoparticles depends on the type of cells and their abilities to defend against stressful conditions.

To find possible molecular mechanisms of AgNPs-mediated cell death, we measured changes in the transcript levels of selected proteins involved in the apoptosis pathway. We observed no increase in p53 expression for any AgNPs concentration used. This observation is consistent with studies of Choi et al. (2006), where despite obvious cytotoxic effects of AgNPs on liver tissue no significant change in p53 mRNA level has been observed. Although another group (Gopinath et al., 2010) showed a slight increase in p53 expression, it is more likely that AgNPs treatment triggers protein activation rather than transcription of p53. Activation of p53 includes p53 phosphorylation followed by cofactor-mediated conformational change. Indeed, we observed weak phosphorylation of p53 in response to AgNPs treatment. Considering quick and transient phosphorylation of p38 after AgNPs addition, we imply that observed p53 phosphorylation might be mediated by activated p38 MAP kinase. This conclusion is supported by the finding that p38 kinase can activate p53 through the phosphorylation of an NH2-terminal regulatory residue, serine 33 (Sanchez-Prieto et al., 2000).

Within known targets of p53 are pro-apoptotic members of Bcl-2 family, including Bcl2-associated X protein (Bax), p53-upregulated modulator of apoptosis (PUMA) and Bcl2-antagonist/killer protein (Bak) (Ghiotto et al., 2010). We observed elevation in the content of mRNAs coding for Bax and PUMA after addition of AgNPs. Choi and co-workers (2010) also showed a statistically relevant increase in mRNA levels of Bax upon AgNPs administration to zebrafish. However, compared to their results, induction of Bax mRNA in our configuration was much weaker. This is probably due to a varying AgNPs concentration used and/or different type of cells analysed.

Analysis of Bak1 expression shows no statistically relevant change in mRNA level. However, neither low increase in Bax expression nor constant Bak expression exclude apoptosis. According to the present state of knowledge, induction of cell death by p53 may occur in a transcription-independent way. This process is initialized by the direct binding to and activation of Bax (Chipuk et al., 2004; Wolff et al., 2008) and Bak (Leu et al., 2004; Pietsch et al., 2008; Wolff et al., 2008), and/or the liberation of Bax/Bak molecules from pre-existing inhibitory complexes with anti-apoptotic proteins, i.e., Mcl-1 (Leu et al., 2004), Bcl-2 and Bcl-xL (Mihara et al., 2003; Chipuk et al., 2004; Tomita et al., 2006).

The studies of Hsin et al. (2008) on NIH3T3 fibroblast treated with 50 and 100 μg/ml of nanosilver powder show that mitochondria-mediated apoptosis was related to a decrease in Bcl-2 at both the protein and mRNA level. In our case, however, Bcl-2 transcript level remains stable. This suggests that in the NHEK cells, AgNPs- driven apoptosis is a result of the action of the apoptotic modulator (i.e., PUMA) rather than the imbalance in the synthesis of anti-apoptotic factors. PUMA is a pro-apoptotic protein and can bind to a wide range of anti-apoptotic Bcl-2 family proteins, which results in the signal transduction towards the initiation of apoptotic processes (Gallenne et al., 2009).

Data suggest that even concentrations of 6.25 μg/ml of AgNPs influence keratinocytes viability. Higher concentrations trigger even more deleterious effects on cell functions. The concentration of AgNPs in commercially available products vary depending on the supplier. According to Lorenz et al. (2012), depending on the origin, socks may contain 18–2925 mg/kg of Ag particles. Assuming that the weight of a sock is around 20 g, this would result in 0.72–117 mg of AgNPs per pair of socks. There are also commercially available skin creams containing concentrations of AgNps as high as 27 μg/ml. The concentration in such products is close to the concentrations used in our study and therefore may result in some toxic effects on treated skin. Nevertheless, we have to mention here that experimental data obtained *in vitro* cannot be compared directly with those done *in vivo*. Keratinocytes present in the skin are surrounded by other type of cells that support their viability and resistance to harmful stimuli.

In summary, we demonstrated that 15 nm PVP-coated AgNPs decreased cell viability and deteriorated proliferative and migratory potential of keratinocytes. We observed significant activation of p38 kinase and weak activation of ERK1/2 and p53 within the first hours of treatment. Furthermore, AgNPs increase caspase 3/7 activity and generate DNA damage. We also observed changes in the expression level of selected transcripts coding for proteins involved in regulation of apoptosis. Our study, for the first time, shows that (depending on the concentration) AgNPs may present possible dangers for primary keratinocytes, concerning the activation of genotoxic and cytotoxic processes. Further detailed experiments are necessary and

should be done directly on the skin to finally clarify the advantages and disadvantages of the use of AgNPs in different products applicable for skin care.

Materials and methods

Silver nanoparticles (AgNPs)

In this study 15 nm silver nanoparticles were used. AgNPs were bought from NANOAMOR (Nanostructured & Amorphous Materials, Inc., Houston, TX, USA). The AgPNs were polyvinylpyrrolidone-coated (PVP) with 25% silver and 75% polymer. The nanopowder was dissolved in a milliQ of water. The concentration was confirmed by means of Inductively Coupled Plasma Atomic Emission Spectroscoy (ICP-AES) as described by Zanette et al. (2011). A lymulus test was used to confirm that the AgNPs solution was free of bacterial endotoxins and endotoxin-like substances.

Cell culture and AgNPs treatment

Proliferating normal human epidermal keratinocytes from adult donors (NHEK) derived from three individuals (Lonza, Basel, Switzerland) were cultured on 75 cm^2 cell culture flasks at 37°C in 5% CO_2 atmosphere in keratinocyte growth medium (Lonza). The culture medium was supplemented with Bovine Pitutary Extract (BPE), human endothelial growth factor (hEGF), insulin (bovine), hydrocortisone, gentamicin- amphotericin-B (GA-1000), epinephrine and transferrin. Twenty-four hours after seeding on multi-well plates, different concentrations of AgNPs (6.25, 12.5, 25 and 50 μg/ml) were added to the cultures and cells were incubated for appropriate time periods.

ATP content assay

Cell viability was analysed by the quantification of intracellular ATP content. NHEKs were plated on 96-wells plates (4×10^3 per well). After 24 h, the cells were treated with different concentrations of AgNPs, previously diluted in a culturing medium to the total volume of 100 μl. ATP content assay was carried out according to the manufacturer's instructions (ATPlite, Luminescence ATP Detection Assay System; PerkinElmer) after 24 h and 48 h of exposure. The luminescence was measured using Infinite M200 microplate reader (Tecan Group Ltd., Männedorf, Switzerland) in three independent experiments, each performed in triplicate. The mean luminescence value for each AgNPs concentration was divided by the mean value for the control cells was thus presented as a percentage of the control (control treated as 100%).

BrdU assay

Cell proliferation was measured with BrdU incorporation assay (Roche). NHEKs were seeded on 96-well plates (3×10^3 per well) and after 24 h cells were treated with different concentrations of AgNPs, previously diluted in a culturing medium to the total volume of 100 μl. BrdU assay was carried out after 24 h and 48 h of culturing with nanoparticles. Cells were incubated with BrdU labeling solution for 12 h (Chemiluminescent Cell Proliferation ELISA, BrdU; Lonza, Basel, Switzerland). Subsequent steps were performed as described earlier (Wegrzyn et al., 2009). Chemiluminescence was measured using an Infinite M200 microplate reader (Tecan Group Ltd., Männedorf, Switzerland) in three independent experiments, each performed in triplicate. The mean luminescence value for each AgNPs concentration was divided by the mean value for the control cells and was thus presented as a percentage of the control (control treated as 100%).

MTT assay

Cell viability was measured using the colorimetric MTT (3-[4,5-dimethylthiazol-2-yl]-2,5-diphenyl-tetrazolium bromide) assay, by monitoring the activity of mitochondrial dehydrogenase. NHEKs were seeded on 96-well plates (4×10^3 per well) and after 24 h cells were treated with AgNPs (as described above). Following 24 h and 48 h stimulation with nanoparticles of Thiazolyl Blue Tetrazolium Bromide (MTT, Sigma Aldrich, St Louis, MO, USA) was added for an additional 3.5 h to the final concentration of 500 ng/ml. The plates were centrifuged at 300 *g* for 5 min at room temperature, the medium was removed and the MTT crystals were dissolved in acidic (40 mM HCl) isopropanol. Absorbance was measured in an Infinite M200 microplate reader (Tecan Group Ltd.) at 570 nm with the reference wavelength of 650 nm. Absorbance of silver nanoparticles in cell culture medium measured in the absence of cells (nanoparticle background) was subtracted from the total absorbance of the nanoparticle-treated cells. Four independent experiments were done, each performed in quintuplicate. The mean absorbance value for each AgNPs concentration was divided by the mean value for the control cells and was thus presented as a percentage of the control (control treated as 100%).

Cell migration

Cell migration was examined with a Leica DMI6000B microscope (Leica Microsystem CMS Wetzlar, Germany) equipped with LAS AF software. NHEKs were seeded on 6-well plates (4×10^4 per well). Twenty four hours and 48 h after the AgNPs addition, the cell movement was recorded for 90 min with a time-lapse of 1.5 min. All experiments were carried out in a humidified atmosphere with 5% CO_2 at 37°C. The tracks of individual cells were determined from the series of changes in the cell central positions, pooled and analysed to determine velocity of cell movement (VCM). All analyses were done using Hiro software v.1.0.0.4 (Miekus and Madeja, 2007). The experiment was performed twice. In each experiment, data was collected for 50 cells. The mean value for 100 cells in each condition was calculated and presented in Figure 2B.

Caspase 3/7 assay

Activity of caspases 3 and 7 was measured using Caspase- Glo 3/7 Assay (Promega, Madison, WI, USA) as described before (Wegrzyn et al., 2009). NHEKs (8×10^3 per well) were seeded on 12-well plates and exposed to 12.5 and 25 ug/ml AgNPs for 24 and 48 h. Protein extracts were isolated with RIPA buffer (Sigma Aldrich) and 3 μg of protein was mixed with 40 μl of Caspase-Glo 3/7 Reagent on a white 96-well plate. After 120 min of incubation, luminescence was measured with

an Infinite M200 microplate reader (Tecan Group Ltd.) in three independent experiments, each performed in duplicate. Mean luminescence value for each AgNPs concentration was divided by the mean value for the control cells and was thus presented as a percentage of the control (control treated as 100%).

Comet assay

The level of DNA damage was tested by electrophoresis of single cells in agarose gel (Singh et al., 1988; Singh et al., 1994; Tice et al., 2000). For the experiment, the cells were plated at the density of 2.1×10^3 cells/cm^2 and treated with 12.5 and 25 ug/ml AgNPs for 24 h and 48 h. Cells were then harvested and washed twice with PBS. In the next step, 10 µl of cell suspension was mixed with 75 µl of 0.5% low melting point agarose (LMPA) preheated to 37°C, dissolved beforehand in PBS without Ca^{2+} and Mg^{2+}. Then cells were deposited on slides and incubated on ice for 5 min. Afterward that, the slides were immersed in cold lysis solution containing 2.5 M NaCl, 0.1 M EDTA, 10 mM Tris, 10% DMSO and 1% Triton X-100, pH 10 and incubated overnight at 4°C. After lysis, the slides were neutralized by rinsing twice in 0.4 M Tris buffer, pH 7.5 and then placed into a horizontal electrophoresis apparatus filled with buffer (1 mM EDTA, 300 mM NaOH, pH>13). After 40 min preincubation (unwinding DNA) electrophoresis was run for 30 min at a fixed voltage of 23 V (0.74 V/cm, 300 mA). After gel electrophoresis the slides were rinsed three times with neutralization buffer (0.4 M Tris pH 7.5; 4°C), fixed with cold 100% methanol for 5 min and then dried at room temperature. Before fluorescent microscope analysis, the slides were washed with distilled water for 5 min and then stained with propidium iodide (2.5 µg/ml). All the steps described above were carried out under only red light to prevent any additional damage. The cells were analysed with a fluorescence microscope (Olympus IX-50) at 400× magnification. Analysis of DNA damages was carried out with the COMET PLUS 2.9 software (Comet Plus, Theta System Gmbh, Germany). For the determination of DNA damage the percentage content of DNA in the comet's tail (%DNA) was used. The data were collected for 50 randomly selected comets from each slide. Three independent experiments were done in two replicates (noumber of cells per each condition=300).

Western blotting

NHEKs were seeded on 60 mm Petri dish (2×10^5 per dish) and then total cell lysates were prepared using RIPA buffer supplemented with protease inhibitors (Sigma Aldrich). From each sample, 25 µg of protein was separated on SDS-Page 10% polyacrylamide gel. Following electrotransfer to PVDF membrane (Merck Millipore, Billerica, MA, USA) and blocking in 2% BSA (BioShop, Burlington, Canada) dissolved in Tris-buffered saline (150 mM NaCl, 20 mM Tris pH 7.6) containing 0.1% Nonidet, the membranes were incubated with primary antibodies at 4°C overnight. The following antibodies and dilutions were used: Akt (1:1000; Cell Signaling, Beverly, MA, USA), Phospho-Akt (1:2000; Cell Signaling), SAPK/JNK (1:500; Cell Signaling), Phospho-SAPK/JNK (1:500; Cell Signaling), p38 MAPK (1:1000; Cell Signaling), Phospho-p38 MAPK (1:500; Cell Signaling), p44/42 MAPK (1:2000; Cell Signaling), Phospho-p44/p42 MAPK (1:1000; Cell Signaling), p53 (1:200; Santa Cruz Biotechnology, Santa Cruz, CA, USA), Phospho-p53 (1:1000; Cell Signaling) and α-tubulin (1:2000; Calbiochem, Merck Group, Darmstadt, Germany). Tubulin was used as a loading control. The following secondary antibodies were used: peroxidase-conjugated anti-rabbit (1:3000–1:10,000; Cell Signaling) and peroxidase-conjugated anti-mouse (1:20,000, BD Pharminogen, Franklin Lakes, NJ, USA). After incubation with secondary antibodies, the chemiluminescence detection was carried out using Luminata Crescendo Western HRP Substrate (Merck Millipore). Membranes were exposed to Kodak Medical X-ray Film (Kodak, New York, NY, USA).

Real-time PCR

Total RNA was isolated using the modified Chomczynski-Sacchi method (Chomczynski and Sacchi, 2006). RNA concentration was measured with a ND-1000 spectrophotometer (NanoDrop, Wilmington, DE, USA) and RNA integrity was verified on a 1% agarose gel.

Number	Gene name and NCBI accession number	Forward/reverse	Sequence
1	BCL2	Forward primer	TCCGCATCAGGAAGGCTAGA
	NM_000633.2	Reverse primer	AGGACCAGGCCTCCAAGCT
2	BCL2L1	Forward primer	GCTTTGAACAGGATACTTTTGTG
	NM_001191.2	Reverse primer	CCACAGTCATGCCCGTCAG
3	BCL2L1	Forward primer	CTGTGCGTGGAAAGCGTAGA
	NM_138578.1	Reverse primer	ACAAAAGTATCCCAGCCGCC
4	BAX	Forward primer	GCTGTTGGGCTGGATCCAAG
	NM_138764.4	Reverse primer	TCAGCCCATCTTCTTCCAGA
5	BAK1	Forward primer	CATCAACCGACGCTATGACTC
	NM_001188.3	Reverse primer	GTCAGGCCATGCTGGTAGAC
6	BBC3	Forward primer	GACCTCAACGCACAGTACGAG
	NM_001127240.1	Reverse primer	AGGAGTCCCATGATGAGATTGT
7	TP53	Forward primer	AGTCTAGAGCCACCGTCCAG
	NM_000546.4	Reverse primer	AGTCTGGCTGCCAATCCAGG
8	BECN1	Forward primer	TAGACCGGACTTGGGTGACG
	NM_003766.3	Reverse primer	TTAGACCCTTCCATCCCTCAGC

Table 1 List of primers used in real-time PCR.

For the real-time PCR experiment, 1 μg of total RNA was reverse-transcribed using oligo(dT) primer and M-MLV reverse transcriptase (Promega). Following synthesis, cDNA was diluted five times and real-time PCR was carried out using Rotor-Gene 3000 (Corbett, Cambridge, UK) system and Sybr Green-based master mix (Finnzymes, Espoo, Finland). After an initial denaturation step for 10 min at 95°C, conditions for cycling were: 40 cycles of 15 s at 95°C, 15 s at 58°C and 20 s at 72°C. The fluorescence signal was measured right after the extension step. To verify specificity of the PCR product a melting curve was generated. As an internal reference, gene β_2 microglobulin (B2M) was used. All samples were run in duplicate. A list of the primers used in the real-time PCR is presented in Table 1.

Statistical analysis

All results are the means of at least three independent experiments±standard deviation (SD). The data were analysed using a Student's *t*-test and only in the case of comet assay data were calculated by RIR Tukey test. Statistical significance was accepted at a level of $p \leq 0.05$.

Acknowledgements: The work described here was supported by the European Community Grant: COST action BM0903 and the Polish Ministry of Science and Higher Education grant: 776/N-COST/2010/0; both awarded to Jolanta Jura. The Faculty of Biochemistry, Biophysics and Biotechnology of the Jagiellonian University is a beneficiary of structural funds from the European Union (grant No: POIG.02.01.00-12-064/08 – 'Molecular biotechnology for health'). We would like to thank Dr. J. Koziel from Microbiology Department of the Faculty of Biochemistry, Biophysics and Biotechnology for performing the microbiological tests.

Received May 15, 2012; accepted September 17, 2012

References

Ahamed, M., Alsalhi, M.S., and Siddiqui, M.K. (2010). Silver nanoparticle applications and human health. Clin. Chim. Acta *411*, 1841–1848.

Arora, S., Jain, J., Rajwade, J.M., and Paknikar, K.M. (2009). Interactions of silver nanoparticles with primary mouse fibroblasts and liver cells. Toxicol. Appl. Pharmacol. *236*, 310–318.

Asare, N., Instanes, C., Sandberg, W.J., Refsnes, M., Schwarze, P., Kruszewski, M., and Brunborg, G. (2011). Cytotoxic and genotoxic effects of silver nanoparticles in testicular cells. Toxicology *291*, 65–72.

Bartkova, J., Gron, B., Dabelsteen, E., and Bartek, J. (2003). Cell-cycle regulatory proteins in human wound healing. Arch. Oral Biol. *48*, 125–132.

Benn, T.M. and Westerhoff, P. (2008). Nanoparticle silver released into water from commercially available sock fabrics. Environ. Sci. Technol. *42*, 4133–4139.

Chaloupka, K., Malam, Y., and Seifalian, A.M. (2010). Nanosilver as a new generation of nanoproduct in biomedical applications. Trends Biotechnol. *28*, 580–8.

Chen, X. and Schluesener, H.J. (2008). Nanosilver: A nanoproduct in medical application. Toxicol. Lett. *176*, 1–12.

Chipuk, J., Kuwana, E.T., Bouchier-Hayes, L., Droin, N.M., Newmeyer, D.D., Schuler, M., and Green, D.R. (2004). Direct activation of Bax by p53 mediates mitochondrial membrane permeabilization and apoptosis. Science *303,* 1010–1014.

Choi, J.E., Kim, S., Ahn, J.H., Youn, P., Kang, J.S., Park, K., Yi, J., and Ryu, D.Y. (2006). Induction of oxidative stress and apoptosis by silver nanoparticles in the liver of adult zebrafish. Aquat. Toxicol. *100*, 151–159.

Chomczynski, P. and Sacchi, N. (2006). The single-step method of RNA isolation by acid guanidinium thiocyanate-phenol-chloroform extraction: twenty-something years on. Nat. Protoc. *1*, 581–585.

Das, S.K., Saha, S.K., Das, A., Halder, A.K., Banerjee, S.N., and Chakraborty, M. (2008). A study of comparison of efficacy and safety of talc and povidone iodine for pleurodesis of malignant pleural effusions. J. Indian Med. Assoc. *106*, 589–590.

Edwards-Jones, V. (2009). The benefits of silver in hygiene, personal care and healthcare Lett. Appl. Microbiol. *49*, 147–152.

Eom, H.J. and Choi, J. (2010). p38 MAPK activation, DNA damage, cell cycle arrest and apoptosis as mechanisms of toxicity of silver nanoparticles in Jurkat T cells. Environ. Sci. Technol. *44*, 8337–8342.

Gallenne, T., Gautier, F., Oliver, L., Hervouet, E., Noël, B., Hickman, J.A., Geneste, O., Cartron, P.F., Vallette, F.M., Manon, S., et al. (2009). Bax activation by the BH3-only protein Puma promotes cell dependence on antiapoptotic Bcl-2 family members. J. Cell. Biol. *185*, 279–290.

Ghiotto, F., Fais, F., and Bruno, S. (2010). BH3-only proteins: the death-puppeteer's wires. Cytometry A *77*, 11–21.

Gopinath, P., Gogoi, S.K., Sanpui, P., Paul, A., Chattopadhyay, A., and Ghosh, S.S. (2010). Signaling gene cascade in silver nanoparticle induced apoptosis. Colloids Surf B Biointerfaces *77*, 240–245.

Hackam, D.J. and Ford, H.R. (2002). Cellular, biochemical, and clinical aspects of wound healing. Surg. Infect. (Larchmt) *3* (Suppl 1), S23–S35.

Henry, G., Li, W., Garner, W., and Woodley, D.T. (2003). Migration of human keratinocytes in plasma and serum and wound re-epithelialisation. Lancet *361*, 574–576.

Hsin, Y.H., Chen, C.F., Huang, S., Shih, T.S., Lai, P.S., and Chueh, P.J. (2008). The apoptotic effect of nanosilver is mediated by a ROS- and JNK-dependent mechanism involving the mitochondrial pathway in NIH3T3 cells. Toxicol. Lett. *179*, 130–139.

Kalishwaralal, K., Banumathi, E., Ram Kumar Pandian, S., Deepak, V., Muniyandi, J., Eom, S.H., and Gurunathan, S. (2009). Silver nanoparticles inhibit VEGF induced cell proliferation and migration in bovine retinal endothelial cells. Colloids Surf. B. Biointerfaces *73*, 51–57.

Kang, K., Lim, D.H., Choi, I.H., Kang, T., Lee, K., Moon, E.Y., Yang, Y., Lee, M.S., and Lim, J.S. (2011). Vascular tube formation and angiogenesis induced by polyvinylpyrrolidone-coated silver nanoparticles. Toxicol. Lett. *205*, 227–234.

Kim, T.H., Kim, M., Park, H.S., Shin, U.S., Gong, M.S., and Kim, H.W. (2012). Size-dependent cellular toxicity of silver nanoparticles. J. Biomed. Mater Res. A *10*, 1033–1043.

Leu, J.I., Dumont, P., Hafey, M., Murphy, M.E., and George, D.L. (2004). Mitochondrial p53 activates Bak and causes disruption of a Bak-Mcl1 complex. Nat. Cell Biol. *6*, 443–450.

Li, D., Diao, J., Zhang, J., and Liu, J. (2011). Fabrication of new chitosan-based composite sponge containing silver nanoparticles and its antibacterial properties for wound dressing. J. Nanosci. Nanotechnol. *11*, 4733–4738.

Lim, D., Roh, J.Y., Eom, H.J., Choi, J.Y., Hyun, J., and Choi, J. (2012). Oxidative stress-related PMK-1 P38 MAPK activation as a mechanism for toxicity of silver nanoparticles to reproduction in the nematode Caenorhabditis elegans. Environ. Toxicol. Chem. *31,* 585–592.

Lin, J.J., Lin, W.C., Dong, R.X., and Hsu, S.H. (2012). The cellular responses and antibacterial activities of silver nanoparticles stabilized by different polymers. Nanotechnology *23*, 065102.

Liu, H.L., Dai, S.A., Fu, K.Y., and Hsu, S.H. (2010). Antibacterial properties of silver nanoparticles in three different sizes and their nanocomposites with a new waterborne polyurethane. Int. J. Nanomedicine *5*, 1017–1028.

Lorenz, C., Windler, L., von Goetz, N., Lehmann, R.P., Schuppler, M., Hungerbühle, K., Heuberger, M., and Nowack, B. (2012). Characterization of silver release from commercially available functional (nano)textiles. Chemosphere *89*, 817–824.

Ma, J., Lü, X., and Huang, Y. (2011). Genomic analysis of cytotoxicity response to nanosilver in human dermal fibroblasts. J. Biomed. Nanotechnol. *7*, 263–75.

Miekus, K. and Madeja, Z. (2007). Genistein inhibits the contact-stimulated migration of prostate cancer cells. Cell. Mol. Biol. Lett. *12*, 348–361.

Mihara, M., Erster, S., Zaika, A., Petrenko, O., Chittenden, T., Pancoska, P., and Moll, U.M. (2003). p53 has a direct apoptogenic role at the mitochondria. Mol. Cell *11,* 577–590.

Park, M.V., Neigh, A.M., Vermeulen, J.P., de la Fonteyne, L.J., Verharen, H.W., Briedé, J.J., van Loveren, H., and de Jong, W.H. (2011). The effect of particle size on the cytotoxicity, inflammation, developmental toxicity and genotoxicity of silver nanoparticles. Biomaterials *32*, 9810–9817.

Piao, M.J., Kang, K.A., Lee, I.K., Kim, H.S., Kim, S., Choi, J.Y., Choi, J., and Hyun, J.W. (2010). Silver nanoparticles induce oxidative cell damage in human liver cells through inhibition of reduced glutathione and induction of mitochondria-involved apoptosis. Toxicol. Lett. *201*, 92–100.

Pietsch, E.C., Perchiniak, E., Canutescu, A.A., Wang, G., Dunbrack, R.L., and Murphy, M.E. (2008). Oligomerization of BAK by p53 utilizes conserved residues of the p53 DNA binding domain. J. Biol. Chem. *283,* 21294–21304.

Sanchez-Prieto, R., Rojas, J.M., Taya, Y., and Gutkind, J.S. (2000). A role for the p38 mitogen-acitvated protein kinase pathway in the transcriptional activation of p53 on genotoxic stress by chemotherapeutic agents. Cancer Res. *60*, 2464–2472.

Singh, N.P., McCoy, M.T., Tice, R.R., and Schneider, E.L. (1988). A simple technique for quantitation of low-levels of DNA damage in individual cells. Exp. Cell Res. *175*, 184–191.

Singh, N.P., Stephens, R.E., and Schneider, E.L. (1994). Modifications of alkaline microgel electrophoresis for sensitive detection of DNA-damage. Int. J. Radiat. Biol. *66*, 23–28.

Sriram, M.I., Kanth, S.B., Kalishwaralal, K., and Gurunathan, S. (2010). Antitumor activity of silver nanoparticles in Dalton's lymphoma ascites tumor model. Int. J. Nanomedicine *5*, 753–762.

Teow, Y., Asharani, P.V., Hande, M.P., and Valiyaveettil, S. (2011). Health impact and safety of engineered nanomaterials. Commun. (Camb.) *47*, 7025–7038.

Tice, R.R., Agurell, E., Anderson, D., Burlinson, B., Hartmann, A., Kobayashi, H., Miyamae, Y., Rojas, E., Ryu, J.C., and Sasaki, Y.F. (2000). Single cell gel/comet assay: guidelines for in vitro and in vivo genetic toxicology testing. Environ. Mol. Mutagen. *35*, 206–221.

Tomita, Y., Marchenko, N., Erster, S., Nemajerova, A., Dehner, A., Klein, C., Pan, H., Kessler, H., Pancoska, P., and Moll, U.M. (2006). WT p53, but not tumor-derived mutants, bind to Bcl2 via the DNA binding domain and induce mitochondrial permeabilization. J. Biol. Chem. *281*, 8600–8606.

Wegrzyn, P., Yarwood, S.J., Fiegler, N., Bzowska, M., Koj, A., Mizgalska, D., Malicki, S., Pajak, M., Kasza, A., Kachamakova-Trojanowska, N., et al. (2009). Mimitin – a novel cytokine-regulated mitochondrial protein. BMC Cell Biol. *10,* 23.

Wolff, S., Erster, S., Palacios, G., and Moll, U.M. (2008). p53's mitochondrial translocation and MOMP action is independent of Puma and Bax and severely disrupts mitochondrial membrane integrity. Cell Res. *18*, 733–744.

Zanette, C., Pelin, M., Crosera, M., Adami, G., Bovenzi, M., Larese, F.F., and Florio, C. (2011). Silver nanoparticles exert a long-lasting antiproliferative effe ct on human keratinocyte HaCaT cell line. Toxicol. In Vitro *25*, 1053–1060.